J. Fluid Mech. (1980), *vol.* 96, *part* 2, *pp.* 275–286
Printed in Great Britain

The nonlinear capillary instability of a liquid jet. Part 2. Experiments on jet behaviour before droplet formation

By K. C. CHAUDHARY

International Business Machines Corporation, General Products Division, San Jose, California

AND T. MAXWORTHY

Departments of Mechanical and Aerospace Engineering, University of Southern California, Los Angeles, California

(Received 30 June 1978 and in revised form 15 May 1979)

The behaviour of a perturbed capillary jet is experimentally determined by studying the jet from the time it emerges from a small hole to the point at which individual droplets of fluid begin to form. Under any particular set of externally applied experimental parameters, i.e. jet velocity, disturbance wavenumber and amplitude, there is a unique, minimum time to this breakup into drops. This characteristic is needed to relate the magnitude of the input voltage to the modulating device and the output velocity perturbation that it produces. Using this relationship we then compare the experimentally produced profiles of jet shape to corresponding ones calculated by using the theory of Chaudhary & Redekopp (1980). The agreement is satisfactory, especially for small values of input voltage. Then, in the neighbourhood of the cut-off wavenumber, we show that the predicted linear growth of the jet profile is also reproduced in the experimental model.

1. Introduction

The instability and breakup of a capillary jet has been investigated extensively in recent years. The earliest theoretical and experimental work is summarized in *The Theory of Sound* (Rayleigh 1945). The dispersion curve computed by him shows that maximum growth rate of an axisymmetrical disturbance occurs at a non-dimensional wavenumber $k_0 = 0{\cdot}697$.

Furthermore, according to linear theory, the cut-off wavenumber, i.e. the wavenumber above which the surface disturbance does not grow, is always one. However, Yuen (1968) and Nayfeh (1970) have shown that the cut-off wavenumber is dependent on the amplitude of the initial disturbance. For an initial velocity perturbation Chaudhary (1977) has shown that for finite disturbance there is no sharp cut-off wavenumber. Rather, there is a cut-off zone, where the growth rate changes from exponential to linear (near $k_0 = 1$) to an oscillatory solution. The cut-off wavenumber ($k = 1$) is found to exist only in the limiting case of an infinitesimal initial disturbance.

Our experimental investigation was motivated by a desire to more completely understand the nonlinear growth of the capillary jet and to correlate the results

0022-1120/80/4363-8190 $02.00

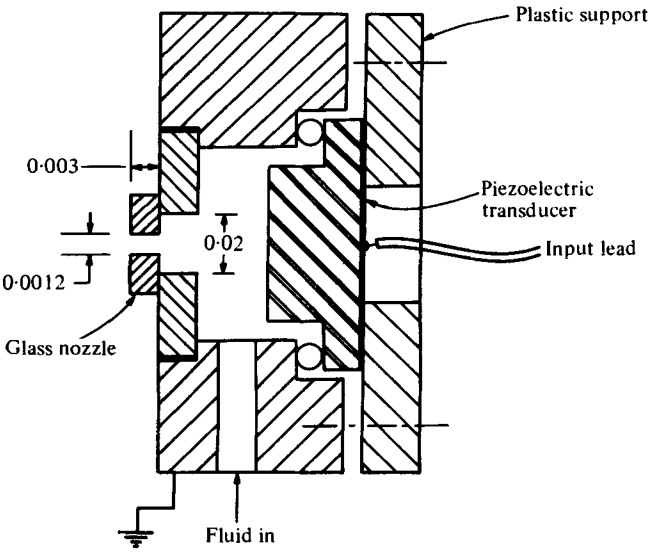

FIGURE 1. Schematic representation of the liquid jet modulator.

with Chaudhary & Redekopp's (1980) theory of the growth of an initial velocity perturbation.

An apparatus was designed to study the nonlinear growth of a capillary jet and its manner of breakup. We wished to study the characteristic of the satellites that are formed and, in particular, to achieve either a desirable satellite configuration or to eliminate them altogether. Enough flexibility was included in the experimental apparatus to enable investigation over a wide range of input parameters, i.e. the amplitudes and wavenumbers of the fundamental and the harmonic inputs and the phase of the harmonic in relation to the fundamental. In this paper only the nonlinear stability of the capillary jet itself is investigated, while in Chaudhary & Maxworthy (1980) the investigation of the production and control of the satellites will be presented.

Section 2 describes the apparatus and the experimental procedure. Section 3 gives the details of the experimental approach and characterization of the jet producing and disturbing device (modulator), while § 4 presents the experimental results and their comparison with theory. Section 5 investigates the jet behaviour in the cut-off zone.

2. Apparatus

Jet modulator

The heart of the system is a device to form the jet and apply a controlled disturbance to it. This is shown schematically in figure 1. Pressurized fluid is fed into a manifold, where periodic disturbances are applied using a piezoelectric transducer with one face in contact with the fluid. The conductivity of the fluid completes the electric circuit.

The jet issues from a round glass nozzle of 0·0012 in. nominal diameter. At the exit plane of the nozzle, it is assumed that the jet is of uniform diameter with the disturbance applied in the form of a velocity perturbance over the mean velocity field.

Control equipment

The overall experimental arrangement is shown schematically in figure 2. A digital logic circuit is used so that a fundamental and a harmonic (2nd or 3rd) can be generated independently and the phase difference between the two can be selected in steps of $\pm 22{\cdot}5°$. These are then used to drive two phase-lock function generators, which give a properly phased sinusoidal output. Relative amplitudes of the fundamental and the harmonic can be individually adjusted and the phase difference can be finely tuned. Once the two wave forms are brought precisely in phase with each other, the digital logic can shift the phase in precise steps of + or $-22{\cdot}5°$. The two wave forms are then summed using an operational amplifier, and the composite signal is then further amplified by a wide-band amplifier, and the amplified signal is fed to the modulator.

A pressurized tank is used to supply liquid at a desired pressure. The air pressure in the tank can be adjusted with the pressure regulator. A $0{\cdot}2\,\mu$m filter removes any contamination from the fiuid. For all the present experiments the pressure of the fluid supplied to the modulator was adjusted to obtain the required jet speed, thereby obtaining the desired wavenumber for a fixed input frequency.

The modulator is mounted on an x, y micrometer stage to facilitate length measurements and observe the jet at various points along its axis. The micrometer stage and the observation equipment are mounted on a heavy Mojave granite optical table to eliminate extraneous vibrations.

Observation technique

For instantaneous observation of the jet, a synchronized light-emitting-diode (LED) stroboscope is used. The pulsed light is received by a television (TV) camera through an amplifying lens system and fed to a TV monitor. The LED is driven by a pulse synchronized to the fundamental wave. To facilitate observation of the jet at different instants, the phase of the LED drive pulse can also be adjusted in relation to the fundamental.

A thin wire mounted on the monitor screen provides a reference point for measurements along the jet axis. The modulator is adjusted at its mounting base to ensure that the jet is in line with the x axis of the micrometer stage; thereafter the length measurements can be made by referring to a fixed point on the TV screen. To measure the breakup distance of the jet, the phase of the LED is adjusted to observe the jet precisely at the instant when the separation point is at a minimum distance from the nozzle exit. To record the shape of the drops and the satellites, photographs were taken from the TV screen using a Tektronix C-10 camera with Polaroid 545 Land Film Holder using Polaroid Type 52 film.

Preparation of the jet fluid

The liquid used in all the experiments was water modified to a small degree by additives. Five gallons of liquid were prepared from $18\,\mathrm{M}\Omega$ de-ionized water and in order to avoid any biological growth, $0{\cdot}1\,\%$ of a commercial bioside (Proxel) was added. For the operation of the particular jet modulator used in the experiments, it was necessary for the fluid to have some conductivity and $0{\cdot}5\,\%$ of sodium nitrate ($\mathrm{Na\,NO_3}$)

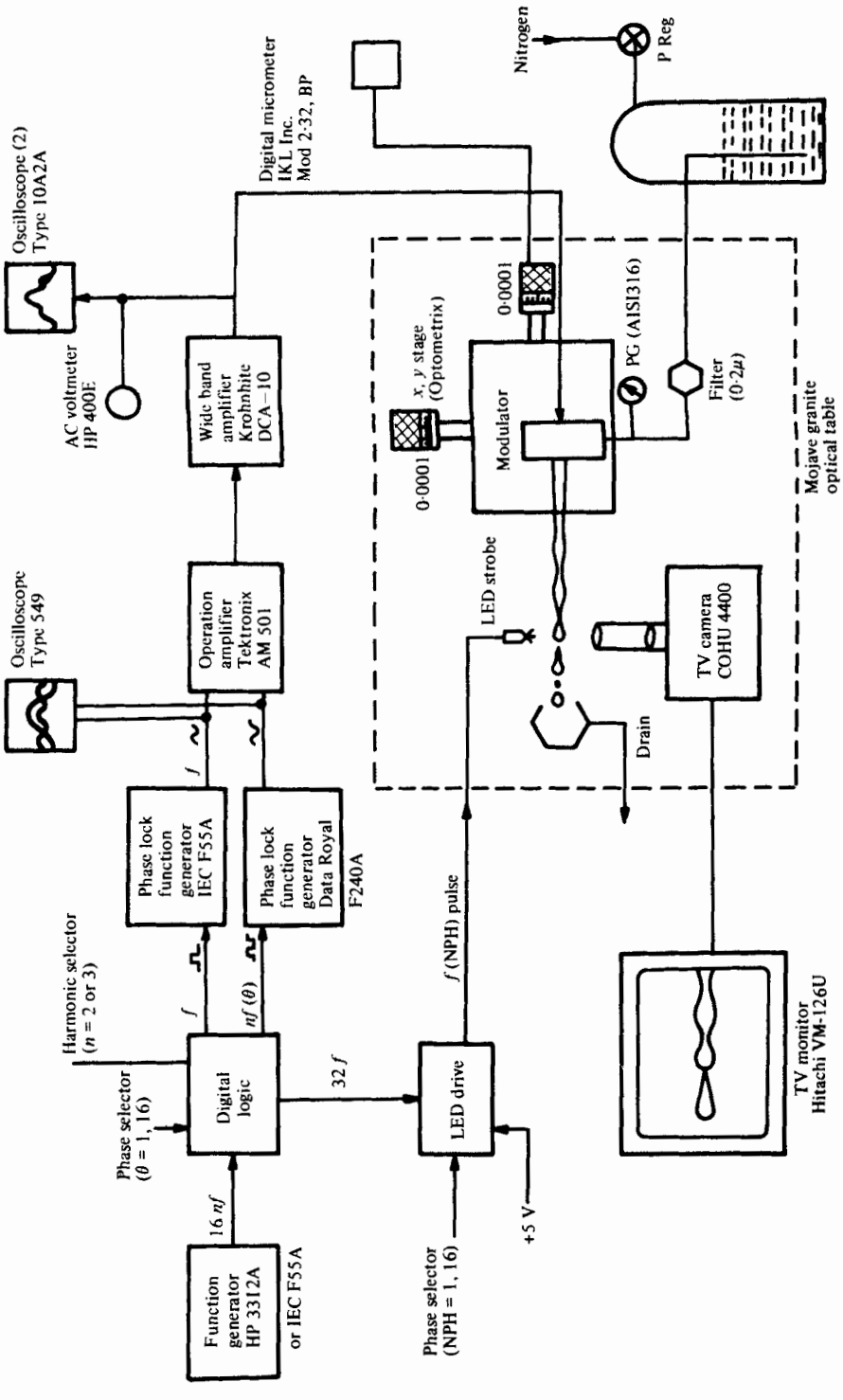

FIGURE 2. Experimental set-up.

was added to provide this. The whole volume of the fluid was filtered through a $0{\cdot}22\,\mu$m filter and then the following properties were measured (at a temperature of 77 °F):

$$\begin{aligned} \text{kinematic viscosity} &= 0{\cdot}911 \times 10^{-2}\,\text{cm}^2\,\text{s}^{-1}, \\ \text{pH} &= 10{\cdot}4, \\ \text{surface tension} &= 65{\cdot}3\,\text{dyn}\,\text{cm}^{-1}, \\ \text{resistivity} &= 167\,\Omega\,\text{cm}^{-1}, \\ \text{specific gravity} &= 1{\cdot}002. \end{aligned}$$

3. Experimental procedure

Measurement of the jet diameter

As a first step the mean diameter of the (undisturbed) jet was determined experimentally. The nozzle had a nominal diameter of 0·0012 in., measured with a precision microscope. A short distance from the nozzle where the jet approached a uniform velocity profile, the jet diameter could be slightly different from the nozzle diameter. The actual value was established by collecting liquid at a known velocity for a known length of time and weighing the liquid on a microbalance. To measure the velocity of the jet, a 100 kHz disturbance was applied to the jet modulator and pressure was adjusted to produce a wavelength of 0·0084 in. The jet velocity was then determined by measuring the length of the first 20 wavelengths from the first discrete drop.† The jet diameter thus established was 0·00153 in. and this value is used in all calculations. It is assumed here that the mean velocity is not affected by the applied disturbances and that the aerodynamic drag on the jet column and droplets is small.

Determination of the modulator characteristics

The input disturbance to the modulator is in the form of a periodic electric potential applied to the piezoelectric transducer. The transducer, in turn, creates pressure and velocity disturbances in the liquid in the manifold. As a result the issuing jet has a velocity disturbance associated with it. To compare the theoretical results to the experiments, it is necessary to relate the magnitude of the applied electric potential to the magnitude of the velocity perturbation within the jet at the nozzle exit.

For present purposes, it was thought most sensible to determine the transfer function of the modulator experimentally, so we treat it as a black box with the electric potential as input and the initial velocity perturbation as output. In general, we can expect that the transfer function will be a function of the operating frequency, applied potential and the wavenumber. Dependence on the frequency will be primarily due to the characteristics of the piezoelectric elements and the structural resonances of the modulator, so to avoid this dependence all the experiments are performed at a fundamental frequency of 100 kHz only. Now, the transfer function can be expected to depend on the applied voltage and wavenumber only.

Assuming that the modulator creates primarily an initial velocity perturbation, an applied voltage (say V_e) will generate a non-dimensional initial perturbation (say ϵ),

† In subsequent experiments, the wavelength is always determined in this way, i.e. the pressure is adjusted till a desired wavelength is obtained.

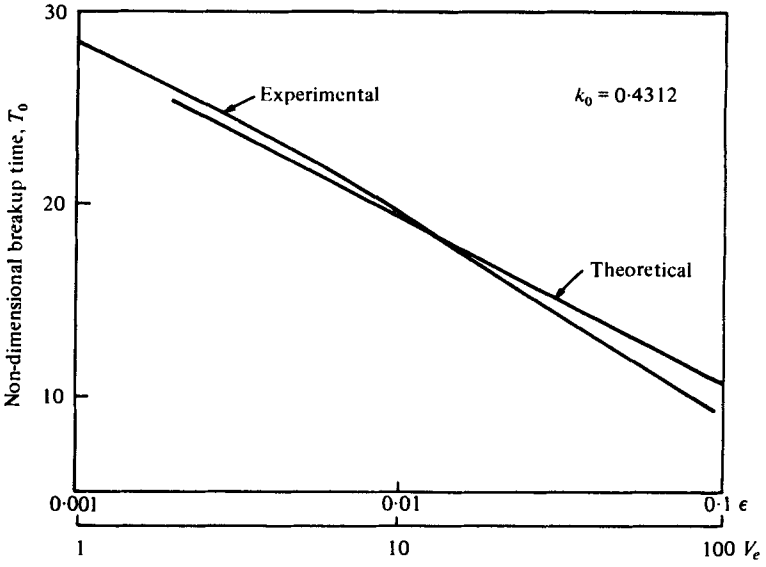

FIGURE 3. Transfer function of the jet modulator at 100 kHz for $k_0 = 0{\cdot}4312$.

when the non-dimensional breakup time T_0 for experimental input V_e is the same as for the theoretical input, ϵ.

Figure 3 shows, on a semi-log graph for a non-dimensional wavenumber $k_0 = 0{\cdot}4312$, the non-dimensional breakup time plotted for the theoretical input ϵ and for the experimental input V_e (V r.m.s.). Examining these plots, one finds that the theoretical breakup time can be approximated on a semi-log plot by a straight line

$$T_0 = 2{\cdot}283 - 8{\cdot}502 \log \epsilon \quad \text{for} \quad k_0 = 0{\cdot}4312, \tag{1}$$†

and the experimentally measured T_0 can be represented on a semi-log plot by a third-order polynomial

$$T_0 = 28{\cdot}290 - 7{\cdot}648(\log V_e) - 1{\cdot}620(\log V_e)^2 + 0{\cdot}306(\log V_e)^3 \quad \text{for} \quad k_0 = 0{\cdot}4312. \tag{2}$$‡

Comparing T_0 from (1) and (2) we find that

$$\epsilon = \exp[-7{\cdot}044 + 2{\cdot}071(\log V_e) + 0{\cdot}439(\log V_e)^2 - 0{\cdot}083(\log V_e)^3] \quad \text{for} \quad k_0 = 0{\cdot}4312. \tag{3}$$

If the modulator is operating away from its sharp resonances, we can expect the form of transfer function to remain the same over some range of operating parameters. In

† A least square approximation is used for equations (1) and (2). For the first order in the linear theory with a velocity perturbation this equation would be

$$T_0 = 2{\cdot}575 - 8{\cdot}454 \log \epsilon.$$

‡ The form of this equation depends on the characteristic of the particular modulator. The modulator used was such that even a straight line

$$T_0 = 28{\cdot}330 - 9{\cdot}785 (\log V_e)$$

would have been a reasonable fit to experimental data. However, using a third-order polynomial the maximum error in the non-dimensional breakup time over the entire data set is less than $\pm 0{\cdot}03$.

such a case the numerical coefficients appearing in (3) will be weak functions of operating frequency and wavenumber.

In fact, figure 3 itself can be used as a transfer function diagram. Drawing a constant T_0 line, the intersection with experimental and theoretical curves gives the corresponding value of V_e and ϵ.

4. Comparison with theory

The transfer function between the disturbance input to the theoretical model (ϵ) and the input to the experimental device has been found by comparing the non-dimensional breakup time calculated from the theory and measured experimentally. Even if the theory were completely erroneous, it would be possible to make this comparison and relate V_e to ϵ. What we need now is an independent check of some other characteristic that will enable us to evaluate the theory rationally. To do this we compute theoretical surface profiles and compare them with the experimentally determined ones. The following typical values of V_e were selected and the corresponding values of ϵ were computed using (3).

V_e ...	2	4	10	20	40
ϵ ...	0·001691	0·003498	0·009889	0·02263	0·05387

Figure 4 (plates 1 and 2) shows the experimental jet profiles for these five values of V_e along with the theoretical jet profiles for the corresponding five values of ϵ. Comparing these figures we find that, for the low initial inputs, the experimental and the theoretical profiles match very well except in the immediate neighbourhood of the breakup. Up to $V_e = 20$ V, the match is good except for the shape of the final drop. The theory correctly predicts the type of satellite separation, as in figures 4 (*a–d*). For $V_e = 40$ V, the comparison is poor over the final wavelength and the mode of breakup is not correctly predicted.

The reasons for these discrepancies between theoretical and experimental results are as follows.

(i) The theoretical solution is an asymptotic one, strictly valid only in the limiting case of $\epsilon \to 0$. Along with this, the assumption is made that the surface disturbance is always small, a condition which clearly does not hold in the neighbourhood of the breakup. This shows two limitations of the theoretical solution: (*a*) for large ϵ the error in the results increases, and (*b*) in the neighbourhood of the breakup point, the solution will show a large error even for small ϵ. Both these limitations show up in the above comparison.

(ii) Perhaps the greater part of the discrepancy, particularly at higher initial input, comes from the fact that the experimental modulator does not have the ideal initial conditions assumed in the theoretical solution. In the theoretical model it was assumed that the jet has a uniform velocity profile at the point of application of the initial disturbance. However, there is a small (finite) length near the exit of the nozzle where the velocity distribution changes rapidly. Considering the order of magnitude of the quantities involved in determining this length, we find that just outside the nozzle the fluid in the thin outer layer is accelerated by a shear force of the order of the shearing force at the nozzle surface. As this thin layer is accelerated from zero velocity to nearly

	ϵ							
k_0	0·002	0·004	0·01	0·02	0·04	0·07	0·1	0·2
0·21	41·801	37·133	30·965	26·297	21·599	17·767	15·288	10·331
0·31	31·196	27·853	23·444	20·014	16·383	12·666	—	—
0·41	26·095	23·444	19·899	17·219	14·589	12·349	10·994	8·458
0·4312	25·231	22·695	19·294	16·729	14·135	12·061	10·735	8·314
0·51	22·579	20·303	17·306	15·029	12·810	11·052	9·928	7·623
0·61	20·447	18·372	15·634	13·545	11·513	9·870	8·833	6·960
0·697	19·452	17·420	14·769	12·752	10·734	9·149	8·141	6·296
0·72	19·380	17·363	14·683	12·665	10·648	9·063	8·054	6·181
0·74	19·409	17·363	14·683	12·665	10·648	9·034	8·025	6·152
0·81	20·187	18·055	15·231	13·069	10·965	9·265	8·228	6·297
0·91	25·144	22·435	18·833	16·124	13·415	11·311	10·014	8·084
0·95	31·628	28·141	23·559	20·101	16·700	14·078	12·550	—

TABLE 1. Theoretical non-dimensional breakup time with fundamental input only. Fundamental frequency is 100 kHz; characteristic time is $T^* = 0{\cdot}694 \times 10^{-5}$ s.

the mean velocity of the jet, the shearing force reduces from maximum to nearly zero, and its length is of the order of the length of the nozzle. When the initial input is small and the breakoff distance is large, this initial length is unimportant. However, when the initial input is large, the growth of the surface waves in this initial length can be large enough to affect the shape of the profile further down stream.

(iii) The modulator generates its own harmonics, i.e. for a pure sinusoidal input voltage, the initial disturbance created on the jet is not monochromatic. This effect is expected to be more important for higher input voltages.

(iv) The theory assumes that the results for the problem of temporal growth can be applied in this case, in which the jet perturbations are actually growing in space. This means that we have ignored certain axial gradients and flows which must become quite important as the breakup point is approached.

In a similar way, the jet modulator characteristics were investigated at several other wavenumbers. Tables 1–3 show these results. Table 1 shows the theoretical non-dimensional breakup times for a set of values of k_0 and ϵ. Table 2 shows the experimental non-dimensional breakup time for similar values of k_0 and a set of V_e. Using these tables, transfer function diagrams (similar to figure 3) for various values of k_0 can be made. Table 3 shows, for various values of k_0, the coefficients of equations similar to (1) and (2), which are calculated from the theoretical and experimental results given in tables 1 and 2.

Investigating the values given in these tables, we arrive at several conclusions.

(i) The theoretical maximum growth rate of the progressive jet occurs at $k_0 = 0{\cdot}697$ (i.e. the maximum value of the slope a_2 in table 3). This is the same as that given by the linear theory of Rayleigh (1945) and the third-order theory of Yuen (1968).

(ii) Table 1 shows that the theoretical minimum non-dimensional breakup time does not occur at $k_0 = 0{\cdot}697$, the wavenumber for the maximum growth rate. This is because the intercept (a_1) appearing in the equation for T_0 is dependent on wavenumber. Figure 5 shows the (theoretical) wavenumber k_0, which gives the minimum breakup time for different initial inputs ϵ. This shows that, as ϵ approaches zero, the

	V_{rms}												
k_0	1	2	4	7	10	15	20	30	40	50	60	70	80
0·31	35·552	32·794	29·542	26·735	24·701	22·537	20·935	18·481	16·935	15·667	14·635	13·788	13·003
0·41	29·136	26·642	23·961	21·646	19·959	18·232	16·985	14·915	13·700	12·681	11·842	11·198	10·619
0·4312	28·313	25·811	23·137	20·909	19·298	17·558	16·376	14·405	13·085	12·100	11·260	10·566	10·052
0·51	25·671	23·406	21·030	19·101	17·746	16·176	15·059	13·272	12·094	11·109	10·317	9·728	9·230
0·61	23·827	21·763	19·613	17·937	16·723	15·387	14·403	12·812	11·561	10·626	9·861	9·230	8·671
0·697	23·085	21·059	18·893	17·297	16·158	14·492	14·173	12·618	11·577	10·772	10·050	9·578	9·093
0·72	22·909	20·834	18·673	17·099	15·998	14·838	14·051	12·535	11·504	10·775	10·159	9·616	9·287
0·74	22·297	20·226	18·037	16·333	15·291	14·042	13·205	11·765	10·722	9·973	9·401	9·077	—
0·81	22·903	20·679	18·423	16·682	15·554	14·345	13·539	12·282	11·315	10·670	10·251	10·122	—
0·91	25·860	23·156	20·380	18·184	16·787	15·190	14·101	12·849	12·213	11·905	11·742	11·778	—
0·95	29·366	26·005	22·473	19·924	18·092	16·317	15·032	13·333	12·521	12·086	11·803	11·803	—
0·99	—	—	30·313	25·430	22·321	19·232	17·339	14·927	13·473	12·675	12·317	12·237	—
1·02	—	—	—	29·366	24·826	20·692	18·381	16·504	13·923	13·011	12·565	12·383	—

TABLE 2. Experimental non-dimensional breakup time with fundamental input only. Fundamental frequency is 100 kHz.

k_0	a_1	a_2	b_1	b_2	b_3	b_4
0·31	−0·396	−11·801	35·548	−8·206	−3·331	0·747
0·41	2·185	−8·856	29·110	−7·407	−2·197	0·512
0·51	2·418	−7·456	25·638	−6·954	−1·042	0·073
0·61	2·084	−6·782	23·819	−6·896	0·268	−0·445
0·697	1·557	−6·610	23·092	−7·061	0·580	−0·397
0·72	1·442	−6·629	22·902	−7·084	0·515	−0·308
0·74	1·392	−6·655	22·295	−6·977	0·068	−0·114
0·81	1·259	−6·991	22·883	−7·158	−0·459	0·289
0·91	1·474	−8·703	25·772	−7·113	−4·073	2·045
0·95	1·050	−11·289	29·283	−9·508	−3·794	2·035

TABLE 3. Coefficients of the approximate equations for the theoretical and experimental non-dimensional breakup time. Generalization of equations (1) and (2) for various values of k_0 gives:

$$T_0 = a_1 + a_2 \log \epsilon;$$
$$T_0 = b_1 + b_2 \log V_e + b_3(\log V_e)^2 + b_4(\log V_e)^3.$$

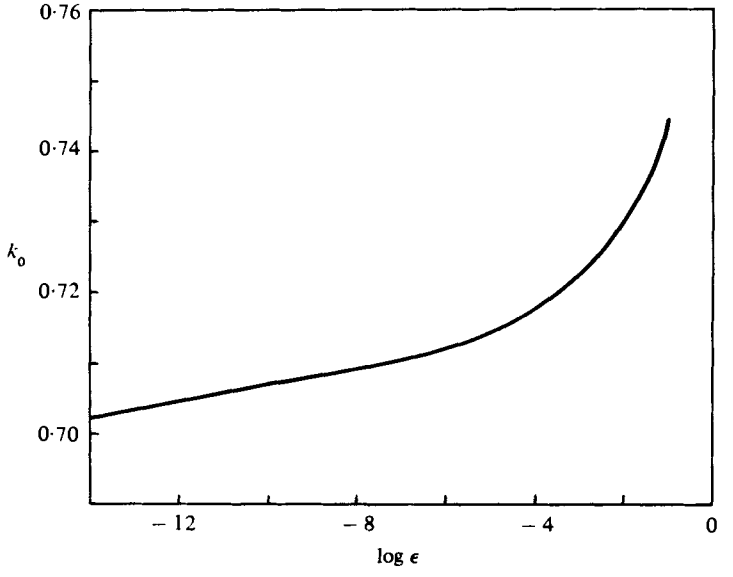

FIGURE 5. Non-dimensional wavenumber k_0 for minimum breakup time as a function of initial input ϵ.

wavenumber for minimum breakup time will approach 0·697 and match the linear theory; otherwise, the minimum breakup time occurs at higher values of k_0.

(iii) Table 2 illustrates that the experimental minimum breakup time always occurs at $k_0 = 0{\cdot}74$. Dependence on the initial inputs cannot be clearly seen in these experimental results. From tables 1 and 2 we observe that the experimental data fall in the range of $\epsilon = 0{\cdot}004$ to 0·1 while figure 5 shows that the theoretical wavenumber for minimum breakup time in this range of ϵ changes from 0·73 to 0·74. It appears that such a small change in the wavenumber could not be detected and a more precise experiment designed to detect this particular phenomenon may be necessary.

(iv) Table 3 indicates that the particular jet modulator used had nearly straight line characteristics at $k_0 = 0{\cdot}74$ (coefficients b_3 and b_4 are very small compared to b_2).

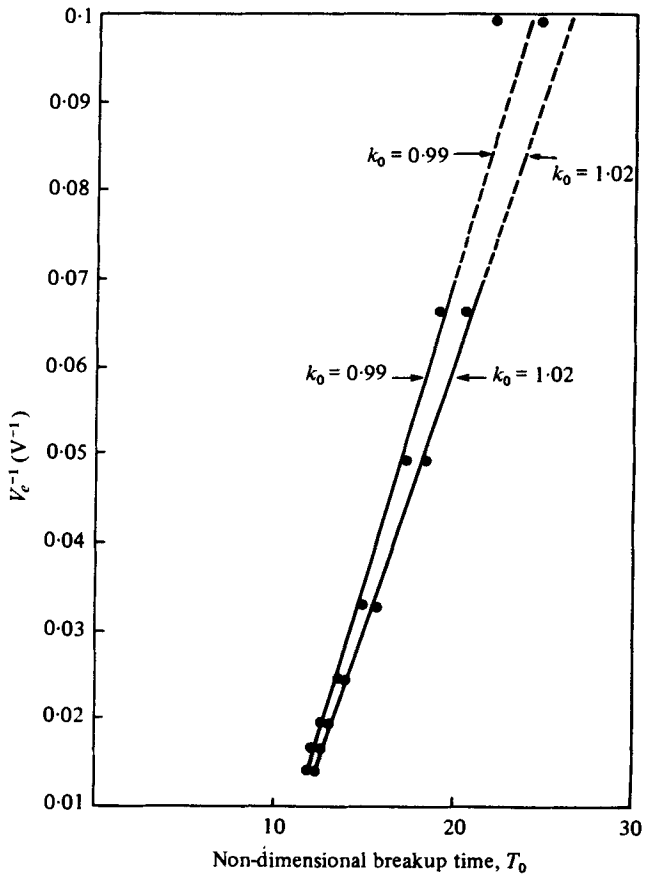

FIGURE 6. Linear growth of the surface waves near $k_0 = 1$.

(v) Table 3 shows the experimental polynomials for $k_0 = 0{\cdot}91$ and $k_0 = 0{\cdot}95$. Large deviations from a nearly straight line representation of T_0 are obvious (i.e. the coefficients b_3 and b_4 are large) at these wavenumbers. This implies that the growth rate near $k_0 = 1$ deviates from the exponential growth rate, as we will show in more detail in the following section.

5. Jet behaviour in the cut-off zone

Two experiments were performed at $k_0 = 0{\cdot}99$ and $1{\cdot}02$, close to the cut-off wavenumber. The non-dimensional breakup time in these cases is also given in Table 2. The theory shows that for large inputs the surface waves grow linearly and that to first order [Chaudhary & Redekopp 1980, equation (31)] this time is given by

$$T_0 = (\omega_0 t)^{-1}.$$

The results of these experiments are shown in figure 6, where T_0 is plotted against the reciprocal of the modulator input voltage V_e. The straight lines in the figure are computed using least square approximation, for data in the range of 15 V to 70 V. In agreement with the theoretical results, the experimental data shows a linear growth rate

for large initial inputs and a transition towards a higher growth rate (i.e. smaller breakup time) for lower inputs (e.g. see data points for $V_e = 10$ in figure 6).

Figure 7 (plate 3) shows the jet profiles at these two wavenumbers for several values of the input voltage. We see that the breakup is not well defined at low inputs but does become well defined for higher values of the input voltages, indicating that there is no sharp cut-off wavenumber.

REFERENCES

CHAUDHARY, K. C. 1977 Ph.D. thesis, University of Southern California.

CHAUDHARY, K. C. & MAXWORTHY, T. 1980 *J. Fluid Mech.* **96**, 287.

CHANDHARY, K. C. & REDEKOPP, L. G. 1980 *J. Fluid Mech.* **96**, 257.

NAYFEH, A. H. 1970 *Phys. Fluids* **13**, 841.

RAYLEIGH, LORD 1945 *The Theory of Sound*. 2nd edn. vol. II, cha. XX. Dover.

YUEN, M. C. 1968 *J. Fluid Mech.* **33**, 151.

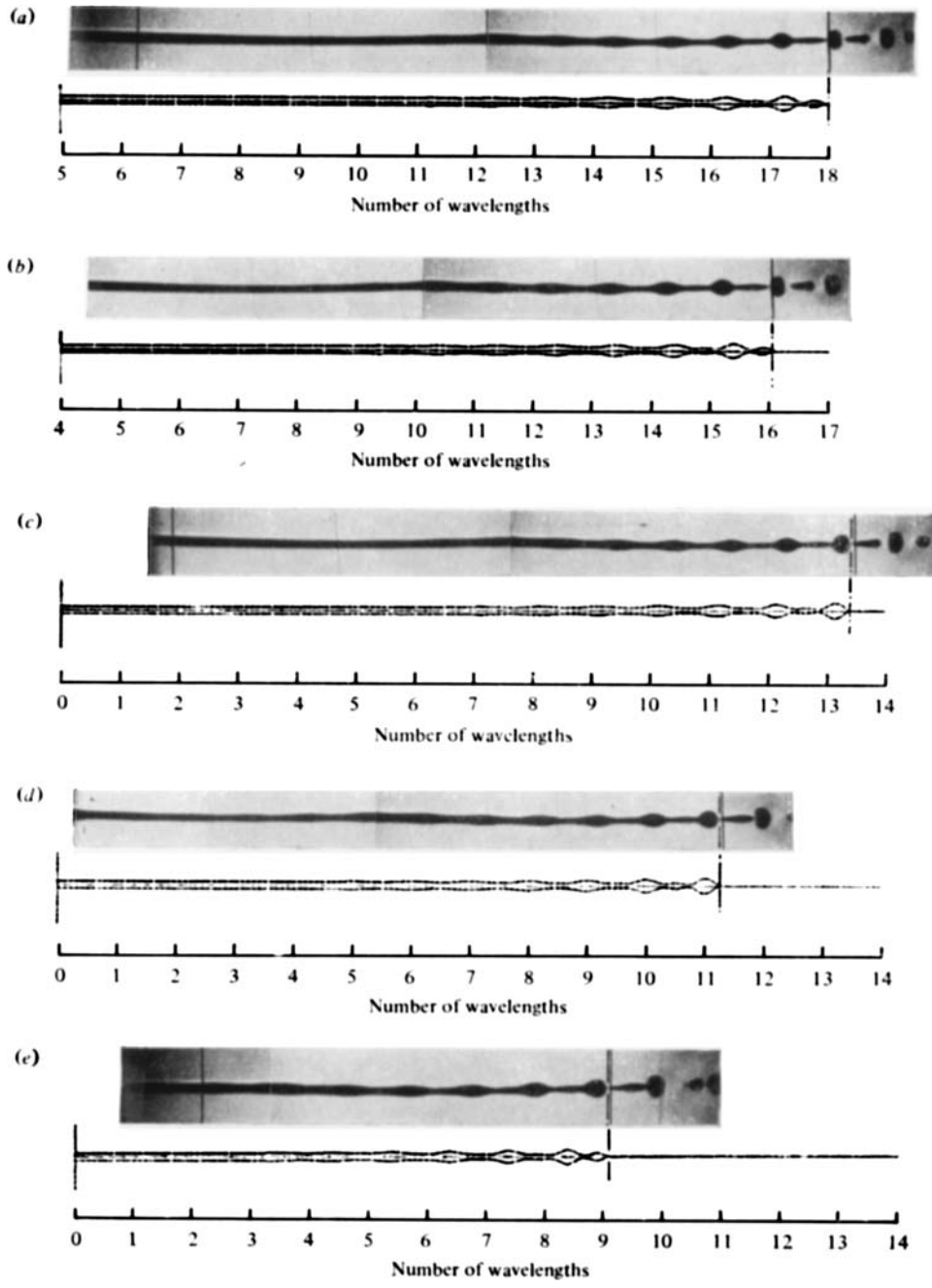

FIGURE 4. Comparison of experimental and theoretical jet profiles with fundamental input alone. $k_0 = 0{\cdot}4312$. (*a*) Experimental profile: $V_e = 2$ V(r.m.s.), non-dimensional breakup time $T_0 = 25{\cdot}83$. Theoretical profile: $\epsilon = 0{\cdot}00169$, $T_0 = 25{\cdot}864$. (*b*) Experimental profile: $V_e = 4$ V (r.m.s.), $T_0 = 23{\cdot}16$. Theoretical profile: $\epsilon = 0{\cdot}00350$, $T_0 = 23{\cdot}18$. (*c*) Experimental profile: $V_e = 10$ V(r.m.s.), $T_0 = 19{\cdot}32$. Theoretical profile: $\epsilon = 0{\cdot}00989$, $T_0 = 19{\cdot}35$. (*d*) Experimental profile: $V_e = 20$ V(r.m.s.), $T_0 = 16{\cdot}30$. Theoretical profile: $\epsilon = 0{\cdot}02263$, $T_0 = 16{\cdot}29$. (*e*) Experimental profile: $V_e = 40$ V(r.m.s.), $T_0 = 13{\cdot}10$. Theoretical profile: $\epsilon = 0{\cdot}05387$, $T_0 = 13{\cdot}10$.

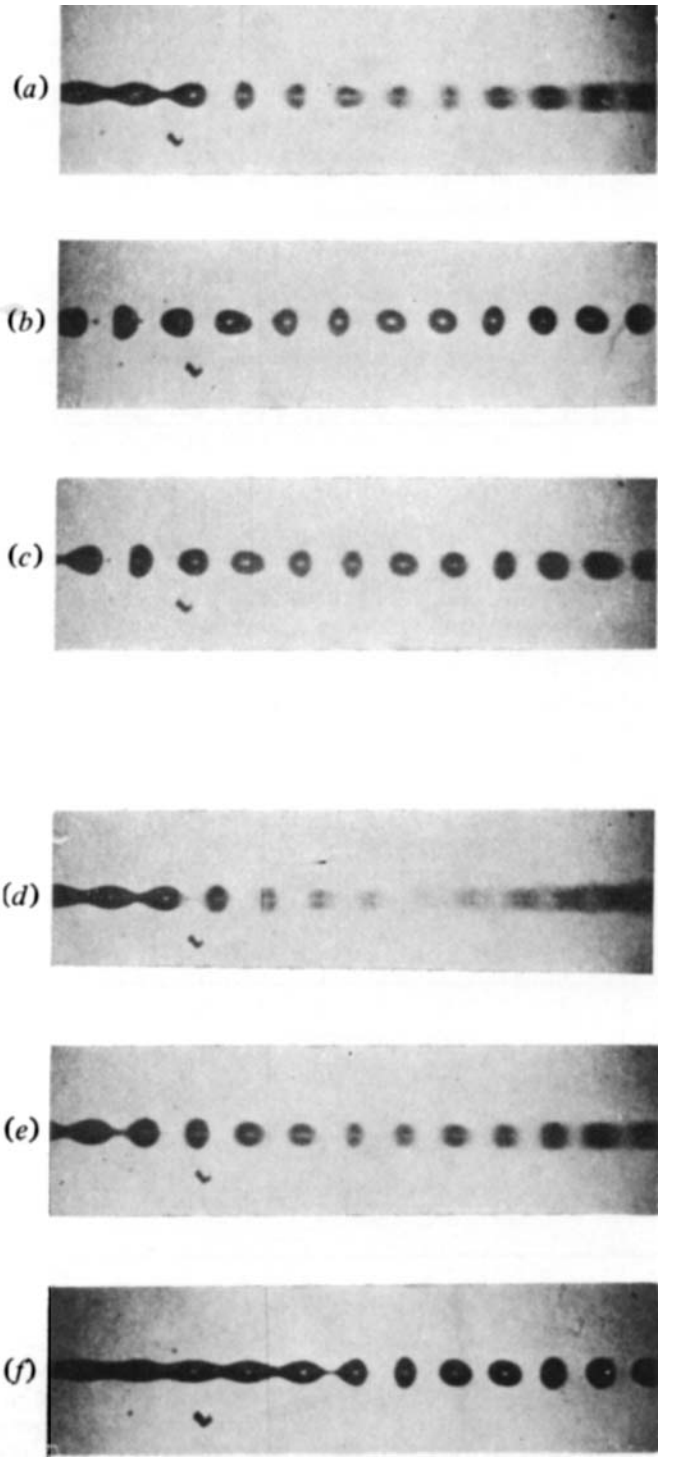

FIGURE 7. Behaviour of the progressive jet in the neighbourhood of $k_0 = 1$. $k_0 = 0{\cdot}99$, fundamental input only: (*a*) $V_e = 7$ V(r.m.s.); (*b*) $V_e = 10$ V(r.m.s.); (*c*) $V_e = 40$ V(r.m.s.). $k_0 = 1{\cdot}02$, fundamental input only: (*d*) $V_e = 7$ V(r.m.s.); (*e*) $V_e = 15$ V(r.m.s.); (*f*) $V_e = 40$ V(r.m.s.). With low initial input, breakup is not well defined, as indicated by fuzziness of the image due to lack of reproducibility in the breakdown process. As the initial input is increased, a well-defined breakup is obtained.